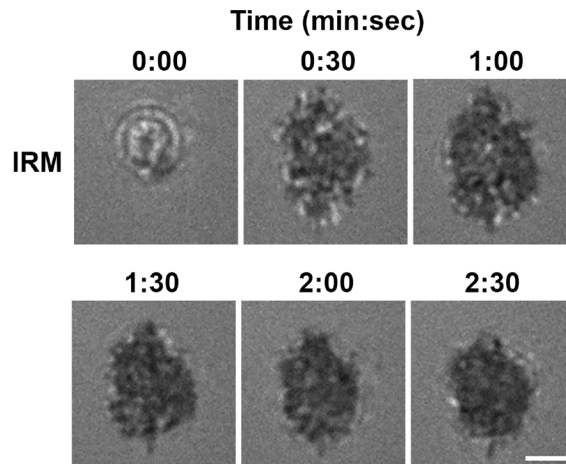


1386 **Supplementary materials for this manuscript include the following:**

1387 7 figures

1388 4 videos

Figure 1-S1



1389

1390 **Figure 1-figure supplement 1. B-cells spread and contract on Fab'-coated-planar lipid**

1391 **bilayers.** Splenic B-cells were pre-warmed to 37°C and incubated with planar lipid bilayers

1392 coated with monobiotinylated Fab' fragment of goat anti-mouse IgG+M (Fab'-PLB) and imaged

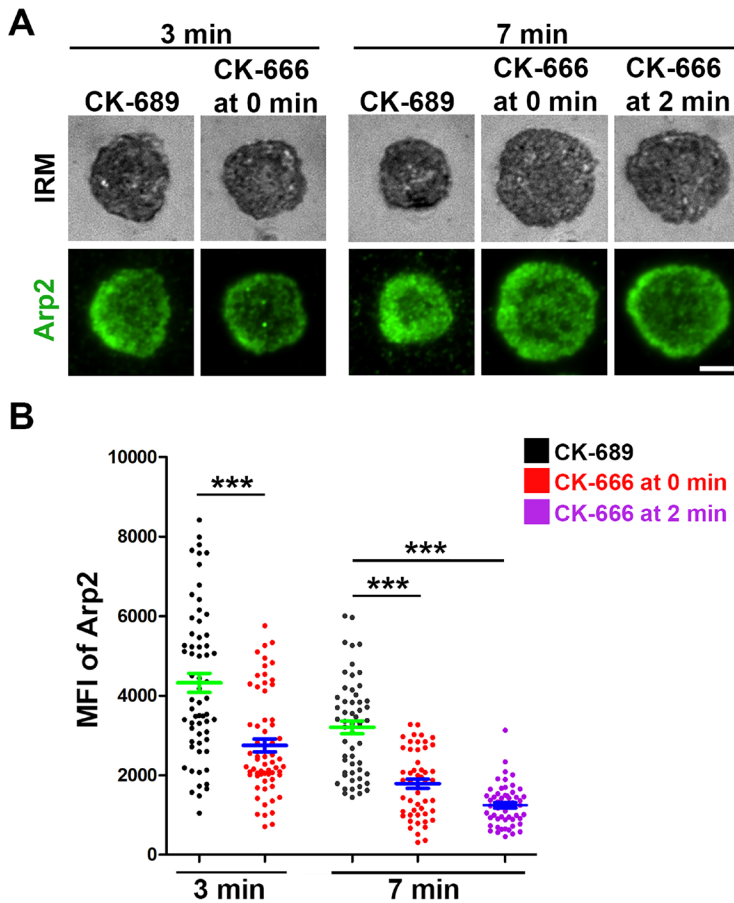
1393 live at 37°C by interference reflection microscopy (IRM). Shown are individual frames from a

1394 time-lapse IRM image of one B-cell. The plasma membrane area contacting with Fab'-PLB (B-

1395 cell contact zone) visualized by IRM increased between 0-1 min after landing, indicating

1396 spreading, and decreased after 1 min 30 sec, indicating contraction. Scale bar, 2 μm.

Figure 1-S2



1397

1398 **Figure 1-figure supplement 2. CK-666 significantly decreases Arp2/3 recruitment to the B-**

1399 **cell contact zone.** WT splenic B-cells were treated with CK-689 or CK-666 (50 μ M) before (0

1400 min) and after maximal spreading (2 min) during incubation with Fab'-PLB at 37°C. Cells were

1401 fixed at 3 and 7 min, permeabilized, stained for Arp2, and imaged using IRM and TIRF. Shown

1402 are representative images (**A**) and the MFI of Arp2 in the contact zone at 3 min and 7 min

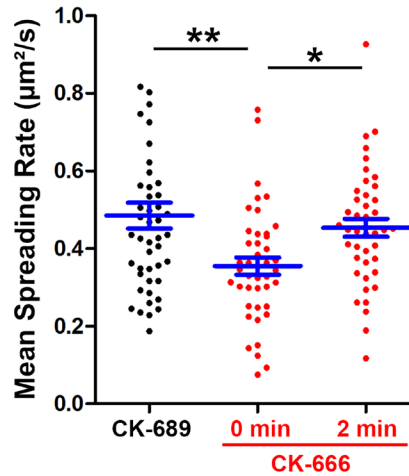
1403 compared between B-cell treated with CK-689 (black dots), CK-666 from 0 min (red dots), and

1404 CK-666 from 2 min (purple dots) (**B**). Data points represent individual cells from 3 independent

1405 experiments with ~20 cells per condition per experiment. Scale bar, 2 μ m. *** $p < 0.001$, by non-

1406 parametric student's t -test.

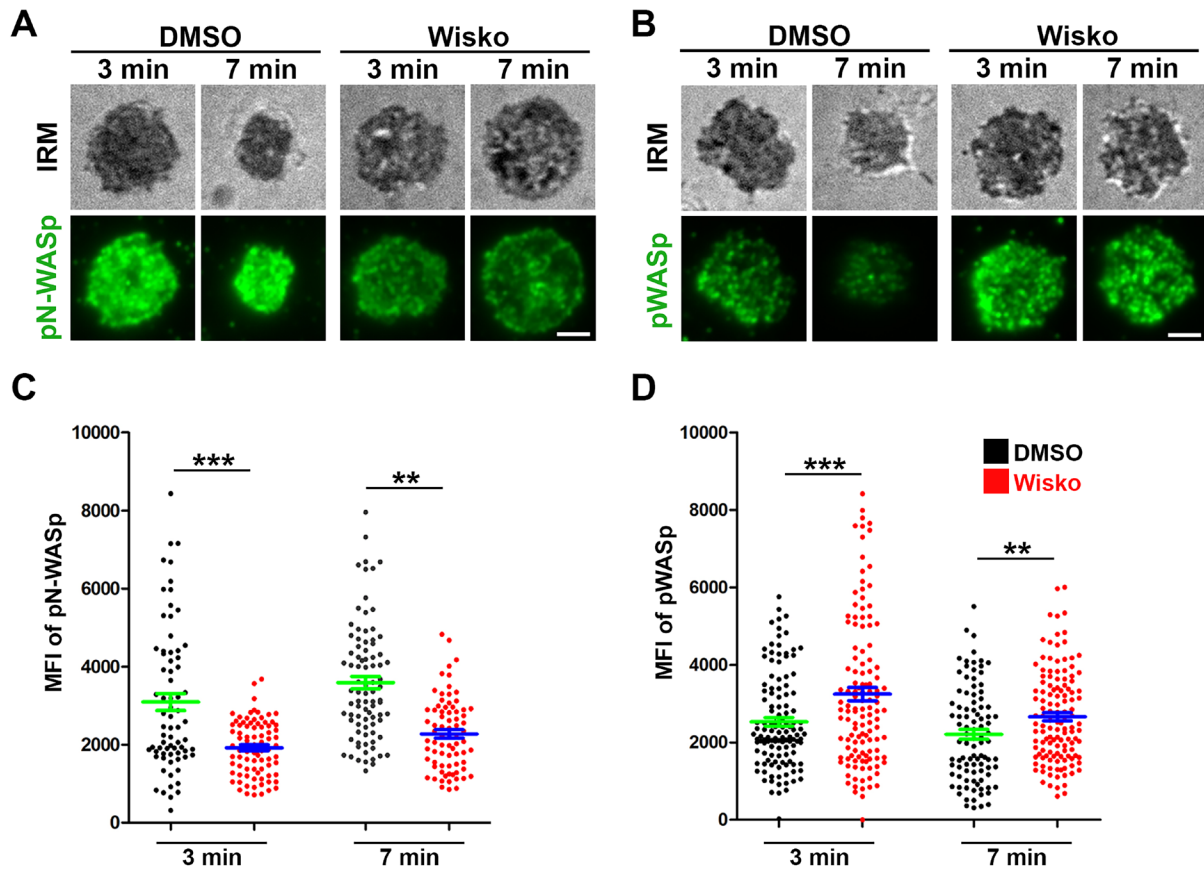
Figure 1-S3



1407

1408 **Figure 1-figure supplement 3. CK-666 treatment before but not after maximal B-cell**
1409 **spreading decreased the spreading kinetics.** WT splenic B-cells were treated with CK-689 or
1410 CK-666 (50 µM) before (0 min) and after maximal spreading (2 min) during incubation with Fab'-
1411 PLB and imaged live at 37°C by IRM. The area occupied by the B-cell contact zone was
1412 measured using IRM images and custom codes made in MATLAB. The mean spreading rate of
1413 each cell during its early spreading phase was quantified using the contact area versus the time
1414 curve of that cell by linear regression. The averaged spreading rates (±SEM) were generated
1415 from 3 independent experiments with ~15 cells per condition per experiment. * $p > 0.05$, **
1416 $p < 0.01$, by non-parametric student's *t*-test.

Figure 1-S4



1417

1418 **Figure 1-figure supplement 4. Wiskostatin treatment inhibits N-WASP activation while**

1419 **enhancing WASP activation in B-cells.** WT splenic B-cells were pre-treated with Wiskostatin

1420 (Wisko, 10 μ M) or DMSO (control) for 10 min at 37°C before and during incubation with Fab'-

1421 PLB. Cells were fixed at 3 and 7 min, permeabilized, stained for phosphorylated N-WASP (pN-

1422 WASP) or WASP (pWASP), and imaged using IRM and TIRF. Shown are representative IRM

1423 and TIRF images of pN-WASP (A) and pWASP (B) at the B-cell contact zone and the MFI

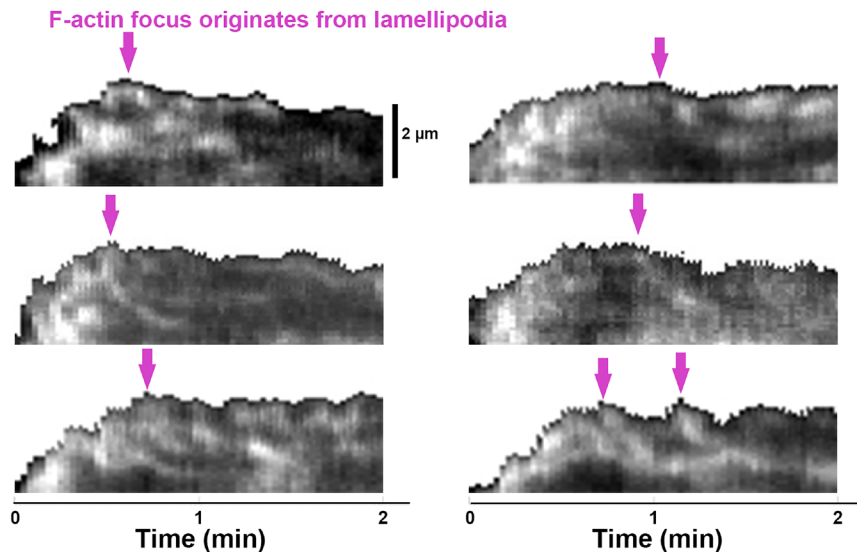
1424 (\pm SEM) of pN-WASP (C) and pWASP (D) in the B-cell contact zone, comparing between DMSO

1425 and Wisko-treated B-cells. Data points represent individual cells from 3 independent

1426 experiments with \sim 25 cells per condition per experiment. Scale bar, 2 μ m. ** $p < 0.01$, ***

1427 $p < 0.001$, by non-parametric student's t -test.

Figure 3-S1

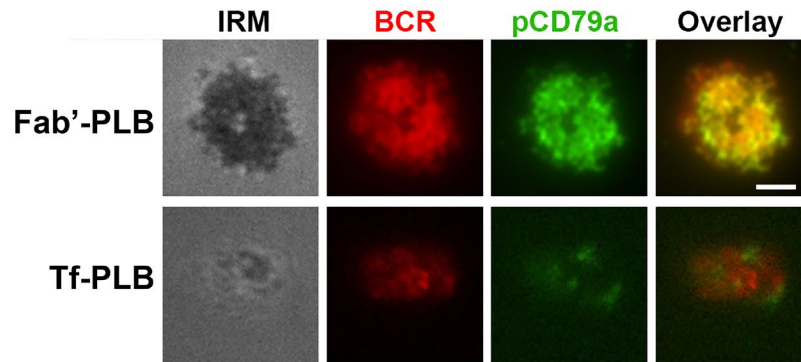


1428

1429 **Figure 3-figure supplement 1. Emerging of Inner F-actin foci from lamellipodia.** Splenic B-
1430 cells from LifeAct-GFP transgenic mice were treated with DMSO, imaged live using TIRF and
1431 IRM during incubation with Fab'-PLB at 37°C, and analyzed using kymographs that were
1432 randomly generated from each cell. Shown are six examples of the kymographs used for
1433 analysis. Arrows indicate the emergence of inner F-actin foci near the lamellipodia.
1434 Lamellipodia-derived inner F-actin foci were identified by their LifeAct-GFP FI ≥ 2 fold of their
1435 nearby region, inside location in the contact zone, migrating away the lamellipodial F-actin, and
1436 trackable for ≥ 8 sec.

1437

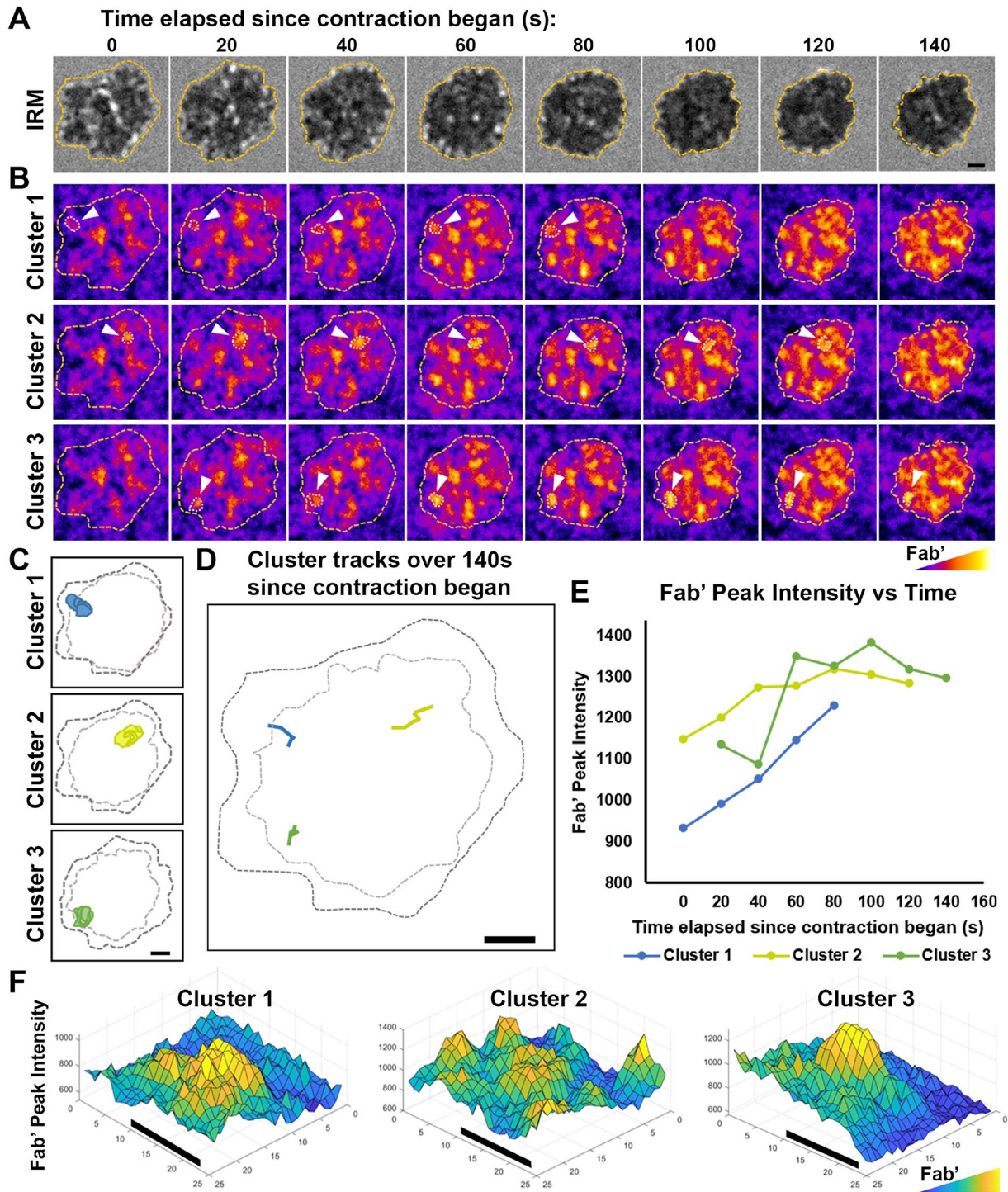
Figure 6-S1



1438

1439 **Figure 6-figure supplement 1. Fab'-PLB, but not Tf-PLB, induces BCR clustering and**
1440 **phosphorylation.** WT splenic B-cells were pre-labeled with Cy3-Fab fragment of goat anti-
1441 mouse IgM+G at a concentration of 2.5 μg per 10^6 cells at 4°C for 30 min, followed by
1442 incubation with Fab'-PLBs or Tf-PLBs for 5 min at 37°C. Cells were fixed, permeabilized,
1443 stained for pCD79a, and imaged using IRM and TIRF. Shown are representative IRM and TIRF
1444 images from three independent experiments. Scale bar, 2 μm .

Figure 6-S2



1445

1446 **Figure 6-figure supplement 2. Tracking and analyzing AF546-Fab' clusters in the B-cell**
1447 **contact zone.** WT splenic B-cells were incubated with AF546-Fab'-PLB at 37°C and imaged
1448 live using IRM and TIRF. Shown are individual frames from time-lapse images of IRM (**A**) and
1449 TIRF (**B**), showing AF546-Fab' clusters within the contact zone of one DMSO-treated (vehicle
1450 control for Wisko) B-cell for 140 sec since the beginning of contraction. Fab' FI is shown as heat
1451 maps using NIH ImageJ. The boundary of the contact zone, detected using IRM images by a
1452 custom MATLAB script, is shown in yellow dashed lines. Arrows point to three representative
1453 clusters among the other clusters detected in the contact zone using custom MATLAB codes.
1454 Cluster detection masks for the three representative clusters are shown (**C**). Moving tracks for
1455 the three AF546-Fab' clusters are shown alongside the initial (black dashed lines) and final state
1456 (gray dashed lines) of the contact zone (**D**). Tracks were generated by following the peak of
1457 AF546 FI in each cluster as it moved. AF546-Fab' peak FI versus time curves for the three
1458 representative clusters are plotted over the duration that each cluster could be detected (**E**).
1459 Surface plots (2.5-D plots) of AF546-Fab' FI show a zoomed-in region consisting of each of the
1460 three AF546-Fab' clusters (**F**). Colors in (**B**) and (**F**) are scaled to AF546-Fab' FI values. Scale
1461 bars, 1 μm .

1462 **Video Legends**

1463 **Figure 1-Video 1. Effects of CK-666, Wiskostatin, conditional N-WASP knockout, and**

1464 **WASP knockout on B-cell contraction.** Splenic B-cells were incubated with planar lipid

1465 bilayers coated with monobiotinylated Fab' fragment of goat anti-mouse IgG+M (Fab'-PLB) in

1466 the absence and presence of various inhibitors and imaged live at 37°C at one frame per 2

1467 seconds by interference reflection microscopy (IRM). Shown are representative IRM time-lapse

1468 images of WT B-cells treated with CK-689 or CK-666 (50 µM) before (0 min) and after maximal

1469 spreading (2 min) (**A**), WT B-cells treated with DMSO or Wiskostatin (Wisko, 10 µM) 10 min

1470 before and during incubation with Fab'-PLB (**B**), B-cells from flox control and B-cell-specific N-

1471 WASP knockout (cNKO) mice (**C**), and B-cells from WT or WASP knockout mice (WKO) (**D**).

1472 The frame in which the contact zone first appears was considered time 0. The videos are sped

1473 up by 20x compared to real time. Scale bar, 2 µm.

1474

1475 **Figure 2-Video 1. Effects of CK-666 and WKO on F-actin foci formation.** Splenic B-cells

1476 from LifeAct-GFP transgenic mice were incubated with Fab'-PLB in the absence and presence

1477 of CK-689 or CK-666 and imaged live at 37°C at one frame per 2 seconds by IRM and total

1478 internal reflection fluorescence microscopy (TIRF). Shown are representative IRM (**A** and **C**)

1479 and TIRF (**B** and **D**) time-lapse images of WT B-cells treated with CK-689 or CK-666 (50 µM)

1480 before and after maximal spreading (**A** and **B**) and WT and WKO B-cells expressing LifeAct-

1481 GFP (**C** and **D**). The video is sped up by 20x compared to real time. Scale bar, 2 µm.

1482

1483 **Figure 5-Video 1. Wiskostatin treatment inhibits NMII ring-like structure formation.** B-cells

1484 from mice expressing GFP fusion of non-muscle myosin IIA (GFP-NMIIA) and LifeAct-RFP

1485 transgenes were treated with DMSO or Wisko (10 µM) 10 min before and during incubation with

1486 Fab'-PLB. The B-cell contact zones were imaged live at one frame per 2 seconds using IRM

1487 and TIRF. Shown are representative IRM and TIRF time-lapse images. The video is sped up by
1488 20x compared to real time. Scale bar, 2 μm .

1489

1490 **Figure 6-Video 1. Inhibition of B-cell contraction reduces the molecular density within**

1491 **BCR clusters.** Splenic B-cells were incubated with AF546-Fab'-PLB in the absence and

1492 presence of various inhibitors and imaged live at 37°C at one frame per 2 seconds by IRM and

1493 TIRF. Shown are representative IRM (**A**, **C**, and **E**) and TIRF (**B**, **D**, and **F**) time-lapse images of

1494 WT B-cells treated with CK-689 or CK-666 (50 μM) before and after maximal spreading (**A** and

1495 **B**), WT B-cells treated with DMSO or Wisko (10 μM) 10 min before and during incubation with

1496 Fab'-PLB (**C** and **D**), and flox control or cNKO B-cells (**E** and **F**). TIRF images (**B**, **D**, and **F**) are

1497 shown as AF546-Fab' FI maps. The video is sped up by 20x compared to real time. Scale bar, 2

1498 μm .